Langmuir Article

pubs.acs.org/Langmuir

Facile Synthesis of Hierarchically Mesoporous Silica Particles with Controllable Cavity in Their Surfaces

Xiaohui Guo, Yonghui Deng, Bo Tu, and Dongyuan Zhao*

Department of Chemistry, Shanghai Key Laboratory of Molecular Catalysis and Innovative Materials, Key Laboratory of Molecular Engineering of Polymers of Ministry of Education and Advanced Materials Laboratory, Fudan University, Shanghai 200433, P. R. China

Received July 1, 2009. Revised Manuscript Received August 29, 2009

Novel and uniform mesoporous silica particles with controllable cavities in their surface have been fabricated using PAA and CTAB as dual templates in a mild reaction system. Herein, a series of hierarchically distinct silica particles can be obtained by simply adjusting the mass ratios (R) of PAA to CTAB. When the R value continues to decrease, the corresponding number and opening size of these cavities are also increased. However, if no PAA added, only unique monodisperse mesoporous silica spheres with uniform size of ~400 nm can be obtained. These specific silica particles were characterized by means of small-angle X-ray diffraction (XRD), scanning electron microscope (SEM), transmission electron microscope (TEM), Fourier-transform infrared (FT-IR) spectra, and nitrogen adsorption−desorption measurements. Results show that these unique mesoporous silica particles totally behave as an hexagonally ordered mesophase. The maximum BET surface area can be as high as 891 m^2/g, and the maximum pore volumes can be as large as 0.27 cm^3/g. Notably, the specific cavity features including opening size and cavity number almost do not change after calcination treatment. Moreover, a possible formation mechanism of the hierarchically distinct silica particles has been put forward, considering that the specific interface instability effect, the reduction in the surface free energy, and the synergic self-assembly of PAA and CTAB in solution can play a key role in mediating the formation of the hierarchical silica nanostructures. In general, the synthesis route is simple and straightforward for the preparation of the other biomineral nanostructures and may play an important role in microencapsulation.

Introduction

Bioinspired morphogenesis of inorganic and inorganic/organic hybrid composites with hierarchically complex architectures directed by self-organized organic superstructures, organic additives, and/or templates has been receiving intense attention due to promising applications in fields such as electronics, catalysts, fine chemicals, biology, and medicine in the past decades.[1−5]

In nature, numerous helical architectures can be formed through the self-assembly of small building blocks into larger macromolecular structures. Recently, much effort has been devoted to the fabrication of inorganic mineral materials, especially for silica materials, due to their hierarchical morphologies. So we can easily explore and apply its power of design and control for the selective preparation of complicated helical chemical architectures.[6,7] In general, the formation of amorphous hydrated silica (biosilica) in living organisms and higher plants is an important process frequently referred to as "biosilicification".[8] Silica, as a mineral material extensively existed in nature, possesses specific aggregate structures and higher chemical activity during the formation process in solution.[9] Therefore, many processes have been developed to explore the synthesis and application of silica-related composites in recent years.[10]

Previous reports show that a great variety of biomolecules or polymers, such as peptides, and long-chain polyamines, chitosan, as well as some synthetic polymers,[11] are involved in the silicification process via specific interactions. It is demonstrated that they could induce the formation of spherical silica particles in the presence of certain siliceous precursors.[12] However, to the best of our knowledge, most studies show that the biomimetic silica materials were formed by using cationic polymers as a soft template in the presence of silicic acid precursor rather than utilizing the direct hydrolytic condensation of alkoxysilanes.[13] Up to now, little work has been done to fabricate silica materials with biomimetic structures in the presence of anionic polymers.

The controlled self-assembly of hierarchically mesoporous silica nanostructures has always been an intense focus in the field of mesoporous materials in recent years. In general, controlling the cooperative self-assembly of organic−inorganic composites is considered to be the dominant factor in the fabrication of mesoporous silica materials.[14] So far, considerable effort[15−17]

*Email: dyzhao@fudan.edu.cn. Tel: 86-21-5566-4194; Fax: 86-21-6564-1740.

(1) Aizenberg, J.; Sundar, V. C.; Yablon, A. D.; Weaver, J. C. *Proc. Natl. Acad. Sci. U.S.A.* **2004**, *101*, 3358.
(2) Sanchez, C.; Soler, G. A. A.; Ribot, F.; Mayer, C.; Cabuil, V.; Lalot, T. *Chem. Mater.* **2001**, *13*, 3601.
(3) (a) Judeinstein, P.; Sanchez, C. *J. Mater. Chem* **1996**, *6*, 511. (b) Aizenberg, J.; Muller, D. A.; Grazul, J. L. *Science* **2003**, *299*, 5610.
(4) Soler-lllia, G. J.; De, A.; Sanchez, C.; Lebeau, B.; Patarin, J. *Chem. Rev.* **2002**, *102*, 4093.
(5) Dujardin, E.; Mann, S. *Adv. Mater.* **2002**, *14*, 775.
(6) (a) Yang, Y.; Suzuki, M.; Fukui, H.; Shirai, H.; Hanabusa, K. *Chem. Mater.* **2006**, *18*, 1324. (b) Yang, Y.; Suzuki, M.; Owa, S.; Shirai, H.; Hanabusa, K. *Chem. Commun.* **2005**, 4462. (c) Kobayashi, S.; Hamasaki, N.; Suzuki, M.; Kimura, M.; Shirai, H.; Hanabusa, K. *J. Am. Chem. Soc.* **2002**, *124*, 6550.
(7) Lin, G.; Tsai, Y.; Lin, H. P.; Tang, C. Y.; Lin, C. Y *Langmuir* **2007**, *23*, 4115.
(8) Perry, C. C.; Keeling-Tucker, T. *J. Biol. Inorg. Chem.* **2000**, *5*, 537.
(9) Minakata, S.; Komatsu, M. *Chem. Rev.* **2009**, *109*, 711.
(10) (a) Aizenberg, J.; Weaver, J. C.; Thanawala, M. S. *Science* **2005**, *309*, 275. (b) Mann, S. Biomimeralization, In *Principle and concepts in bioinorganic materials chemistry*; Oxford University Press: Oxford, 2001.
(11) Pohnert, G. *Angew. Chem. Int. Ed* **2002**, *41*, 3167.
(12) (a) Sumper, M.; Brunner, E. *Adv. Funct. Mater.* **2006**, *16*, 17. (b) Wenzl, S.; Deutzmann, R.; Hett, R.; Hochmuth, E.; Sumper, M. *Angew. Chem. Int. Ed.* **2004**, *43*, 5933.
(13) (a) Sumper, M.; Lorenz, S.; Brunner, E. *Angew. Chem. Int. Ed.* **2003**, *42*, 5192. (b) Knecht, M. R.; Wright, D. W. *Langmuir* **2004**, *20*, 4728.
(14) Sen, T.; Gordon, J. T. T.; Casci, J. L.; Anderson, M. W. *Angew. Chem. Int. Ed.* **2003**, *42*, 4649.

has been made to develop the mesostructured silica materials with various morphologies. These studies may also shed light on fundamental biomineralization mechanisms of silica mineral. Mesoporous silica particles as a hierarchically specific nanostructure are of significant interest due to the extensive applications in drug delivery and controlled release, biology separation, catalysis, and as nanoreactors.[16] Moreover, most of the porous silica particles and hollow spheres have been fabricated by employing hard templates, vesicles, emulsion, and nanoparticles as sacrificial templates. As reported by a previous study on the surfactant involved sol−gel process, monodisperse gigantic hollow mesoporous silica spheres can be formed by simply adjusting the volume ratios of water to ethanol.[18] It is noteworthy that gigantic hollow silica spheres composed of primary mesoporous silica particles have been fabricated in polyethylene oxide-*block*-polypropyl oxide-*block*-polyethylene oxide ($EO_{76}-PO_{29}-EO_{76}$)/butanol/ethanol/water quaternary emulsion reaction system.[19] Chen et al.[20] synthesized porous silica particles and spheres via a dynamic self-assembly route, using ethyl ether and 2-ethoxyethanol as cosolvent and soft template, respectively. Moreover, Lim et al. fabricated a multifunctional silica nanocapsule with a single hole on its surface that is attributed to the emulsion-mediated diffusion process.[21]

To date, most of the reported hollow mesoporous silica spheres and macrospheres with size of ∼15 mm are synthesized by using cationic surfactant cetyltrimethyl ammonium bromide (CTAB) or triblock copolymer ($EO_{76}-PO_{29}-EO_{76}$) with *n*-butanol as cosolvent.[22] More interestingly, Yang et al.[23] synthesized helical mesoporous silica rods with chiral channels by using perfluorooctanoic acid (PFOA) and CTAB as cosurfactants. This unique helical structure is considered to be the result of the reduction in the surface area and surface free energy. Nevertheless, to the best of our knowledge, facile synthesis of mesoporous silica nanocapsule with tailored surface textures utilizing anionic-type surfactants as dynamic template remains a challenge until now.

Poly(acrylic acid) (PAA), an anionic water-soluble polymer molecule, has been extensively adopted as modifier or template for the biomineralization process because it possesses a strong interaction effect and hydrophilic carbonyl groups.[24] It was reported that PAA can modulate the formation of hydroxyapatite ($Ca_5(PO4)_3OH$, HAP) crystals by virtue of the specific adsorption mode between PAA and crystal planes of HAP precursors.[25,26] Sakamoto et al.[27] have successfully synthesized calcium carbonate thin film with periodic patterns in the presence of PAA polymers with different molecular weights as modifier at mild conditions. Moreover, as for silica mineral, there is literature indicating that amorphous silica particles can be readily obtained by combination of polyaminoamide dendrimers and PAA molecules[28] because the PAA can act as a hindrance agent during the formation of silica. However, until now, little work has been done to synthesize mesoporous silica particles by using PAA as modifier during the biomineralization process.

In the present study, for the first time we make use of a combination of the biomineralization process and dynamic template self-assembly[29] between PAA and CTAB for the preparation of mesoporous silica particles with varied cavities in their surfaces at mild reaction conditions. Herein, several kinds of silica samples with controlled surface cavities can be obtained by adjusting the mass ratios of PAA to CTAB (R). Moreover, the possible formation mechanism of this hierarchically mesoporous silica will be discussed in context. Additionally, the facile and simple synthesis strategy that combines the self-assembly and biomineralization can be used to prepare other non-silica-based mesostructures with specific morphologies and nanoarchitectures.

Experimental Section

Preparation of Hierarchical Mesoporous Silica Particles. In a typical synthesis, a certain amount of CTAB was dissolved in mixed solvents containing 20 mL of water and 35 mL of isopropanol. The resulting solution was homogenized for 1 h under magnetic stirring. Separately, a desired amount of PAA (M_n = 200 000) was dissolved in a mixed solvent containing 20 mL of water and 85 mL of isopropanol. Afterward, the above two solutions were mixed and stirred for 0.5 h at 40 °C to form a homogeneous solution. To this solution, 0.45 mL of tetraethyl orthosilicate (TEOS) and 1 mL concentrated ammonia were added. The mixture was further stirred for 24 h. The resulting products were collected by filtration and washing three times with water and ethanol, respectively, and then dried at room temperature. The templates were removed by calcination at 550 °C for 5 h to obtain final silica samples. For the as-synthesized silica samples with different R values, such as R = 2.4, 1.2, 0.6, 0.3, and 0, the corresponding amounts of PAA and CTAB added in the reaction solution can also be seen in Table 1; herein, other experimental parameters were the same as those mentioned above.

Characterizations. Powder X-ray diffraction (XRD) patterns were recorded on a Bruker D4 X-ray diffractometer (Germany) with Ni-filtered Cu KR radiation (40 kV, 40 mA). Fourier-transform infrared (FT-IR) spectra were collected on Nicolet Fourier spectrophotometer using KBr pellets (USA). Nitrogen sorption isotherms were measured at 77 K with a Micromeritcs Tristar 3000 analyzer (USA). Before measurements, the samples were degassed in a vacuum at 180 °C for at least 6 h. The Brunauer−Emmett−Teller (BET) method was utilized to calculate the specific surface areas (S_{BET}) using adsorption data in a relative pressure range from 0.18 to 0.35. By using the Barrett−Joyner−Halenda (BJH) model, the pore volumes and pore size distributions were derived from the adsorption branches of isotherms, and the total pore volumes (V_t) were estimated from the adsorbed amount at a relative pressure P/P_0 of 0.992. Scanning electron microscopy (SEM) images were taken with a Philips XL30 electron microscope operating at 20 kV. Field emission scanning microscopy (FE-SEM) was taken with Hitachi S-4800

(15) (a) Stein, A. *Adv. Mater.* **2003**, *15*, 763. (b) Hampsey, J. E.; Arsenault, S.; Hu, Q. Y.; Lu, Y. F. *Chem. Mater.* **2005**, *17*, 2475.
(16) (a) Bao, X. Y.; Zhao, X. S. *J. Phys. Chem. B* **2005**, *109*, 10727. (b) Kim, T. W.; Kleitz, F.; Paul, B.; Ryoo, R. *J. Am. Chem. Soc.* **2005**, *127*, 7601. (c) Lin, H. P.; Mou, C. Y. *Acc. Chem. Res.* **2002**, *35*, 927.
(17) (a) Kosuge, K.; Sato, T.; Kikukawa, N.; Takemori, M. *Chem. Mater.* **2004**, *16*, 899. (b) Yao, B.; Fleming, D.; Morris, M. A.; Lawrence, S. E. *Chem. Mater.* **2004**, *16*, 4851. (c) Hentze, H. P.; Raghavan, S. R.; McKelvey, C. A.; Kaler, E. W. *Langmuir* **2003**, *19*, 1069.
(18) Zhang, H. J.; Wu, J.; Zhou, L. P.; Zhang, D. Y.; Qi, L. M. *Langmuir* **2007**, *23*, 1107.
(19) Sun, Q. Y.; Magusin, P. C. M. M.; Mezari, B.; Panine, P.; Santen, R. A. V.; Sommerdijk, N. A. J. M. *J. Mater. Chem.* **2005**, *15*, 256.
(20) Chen, H. M.; He, J. H.; Tang, H. M.; Yan, C. X. *Chem. Mater.* **2008**, *20*, 5894.
(21) Lim, Y. T.; Kim, J. K.; Noh, Y. W.; Cho, M. Y.; Chung, B. H. *Small* **2009**, *5*, 324.
(22) Stevens, W. J. J.; Lebeau, K.; Mertens, M.; Van, Tendeloo, G.; Cool, P.; Vansant, E. F. *J. Phys. Chem. B* **2006**, *110*, 9183.
(23) Yang, S.; Zhao, L. Z.; Yu, C. Z.; Zhou, X. F.; Tang, J. W.; Yuan, P.; Chen, D. Y.; Zhao, D. Y. *J. Am. Chem. Soc.* **2006**, *128*, 10460.
(24) (a) Homeijer, S. J.; Olszta, M. J.; Barrett, R. A.; Gower, L. B. *J. Cryst. Growth* **2008**, *310*, 2938–2945. (b) Yu, S. H.; Cölfen, H. *J. Mater. Chem.* **2004**, *14*, 2124.
(25) Buke, E. M.; Guo, Y.; Colon, L.; Rahima, M.; Veis, A.; Nancollas, G. H. *Colloids Surf., B: Biointerface* **2000**, *17*, 49–57.
(26) Iwatsubo, T.; Kusumocahyo, S. P.; Kanamori, T.; Shinbo, T. *J. Appl. Polym. Sci.* **2006**, *100*, 1465.
(27) Sakamoto, T.; Oichi, A.; Sugawara, A.; Kato, T. *Chem. Lett.* **2006**, *35*, 310.
(28) Pouget, E.; Dujardin, E.; Cavalier, A.; Moreac, A.; Valery, C.; Marchi-Artzner, V.; Weiss, T.; Renault, A.; Paternoster, M.; Artzner, F. *Nat. Mater.* **2007**, *6*, 434.
(29) Im, S. H.; Jeong, U.; Xia, Y. N. *Nat. Mater.* **2005**, *4*, 671.

operating at 1.5 kV. A thin gold film was sprayed on the sample before the characterization. Transmission electron microscopy (TEM) images were conducted on a JEOL 2011 microscope (Japan) operated at 200 kV. The sample for TEM measurements was suspended in ethanol and supported on a holey carbon film on a copper grid.

Results and Discussion

By changing the mass ratios (R) of PAA to CTAB, several different silica nanostructures can be obtained. For convenience, the samples synthesized at R values of 0, 0.3, 0.6, 1.2, and 2.4 were referred to as S0, S1, S2, S3, S4, respectively. The SEM images of the obtained samples were summarized in Figure 1. Spherical silica particles with only one surface cavity can be obviously observed when the mass ratio of PAA to CATB is 2.40 (Figure 1a), the diameter of the as-made silica sphere (S4) ranges from 200 to 500 nm, and the maximum opening size of the cavity in its surface can reach to 100 nm. As the mass ratio decreased to 1.20, a novel distorting bread-ring-shaped silica particle can be obtained (Figure 1b), and these particles tend to aggregate with each other. The cavity size of the S3 sample determined from the SEM image appears to be close to that of S4 (Figure 1a). More interestingly, when the mass ratio of PAA to CTAB decreased to 0.60, a class of silica particles with a larger surface cavity size can be observed (Figure 1c,d). From Figure 1d, it can obviously be seen that the maximum opening size of the cavity is up to 260 nm. The unique silica particle is similar to the polystyrene hollow sphere with a big open hole reported in previous literature.[29] Notably, when the R value further decreased to 0.30, a novel sponge-like silica nanostructure with multiple cavities on its surface can be formed (Figure 1e). The maximum opening size of the cavities was calculated to be ~230 nm, and the diameter of the as-made silica particles was in the range of 150−580 nm. In contrast, monodisperse solid silica spheres (S0) with mean diameter of ~400 nm were obtained when no PAA is added ($R = 0$) (Figure 1f), and no cavity can be found in their surface.

Table 1. Summary of the Different Amounts of PAA and CTAB Added with R Value Change in Reaction Solution

R value	[PAA]/ g	[CTAB]/ g
2.4	0.44	0.18
1.2	0.44	0.36
0.6	0.22	0.36
0.3	0.11	0.36
0	0	0.18

At the same time, when the R value is further increased to 4.44, a novel cucurbit-like silica structure with rough surface feature can be formed (Supporting Information Figure S1), the average length of the antenna of the cucurbit is about 80 nm. As mentioned above, although we have investigated the effect of the R value on the morphologies of the as-synthesized silica particles, it is necessary to further explore the influence of the interplay between PAA and CTAB on the morphological evolution of the as-synthesized silica samples, which is helpful to optimize the present synthesis condition. Herein, when the amount of PAA added was kept the same at ~0.10 g, only changing the amount of CTAB added in solution, we can obtain silica samples with different morphologies (Supporting Information Figure S2); namely, the as-synthesized silica samples can evolve from similar spherical to pome-like aggregates, and then to short rods while gradually decreasing the amount of CTAB added from 0.40 to 0.14, and finally to 0.06 g. In contrast, when keeping the amount of CTAB added constant at ~0.10 g, we can also obtain silica samples with distinct morphologies, while only adjusting the amount of PAA added. Herein, when the amount of PAA used is 0.40 g, a kind of irregular particle aggregate with a surface cavity can be observed (Supporting Information Figure S3a); when the amount of PAA added is increased to 0.6 g, smaller-sized particle aggregates can be obtained (Supporting Information Figure S3b); by further increasing the amount of PAA added to 0.8 g, it was found that the morphology of the as-synthesized silica sample shows almost no change (Supporting Information Figure S3c). The results show that the redundant PAA molecule cannot involve and influence the formation of the silica particles. Therefore, the proper mass ratio (R) between PAA and CTAB is a key factor in mediating the morphosynthesis of the as-synthesized silica samples.

After calcination at 550 °C for 5 h, all the silica samples have well-retained morphologies similar to their parent as-made samples. Because of the removal of PAA and CTAB, these silica samples show porous features as revealed by the TEM images (Figure 2). For the calcined sample S3 with R value of 2.40, a

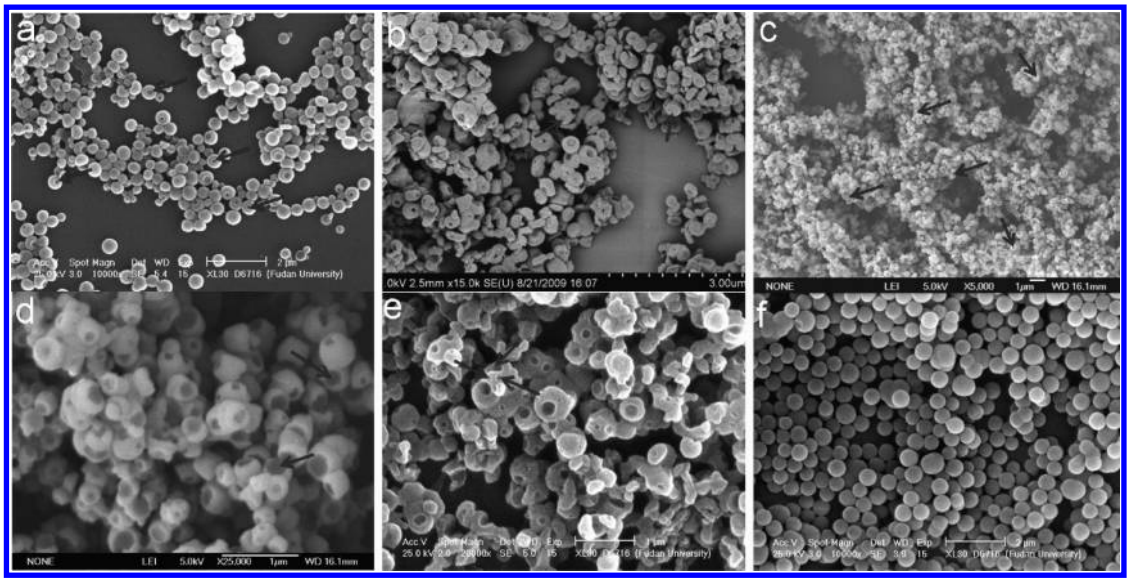

Figure 1. SEM images of distinct silica nanostructures synthesized at different R values. (a) 2.4, (b)1.2, (c, d) 0.6, (e) 0.3, (f) 0. Herein, arrows denote the presence of a cavity on the sample surface. Herein, arrows denote the opening of the cavities on the particle surface.

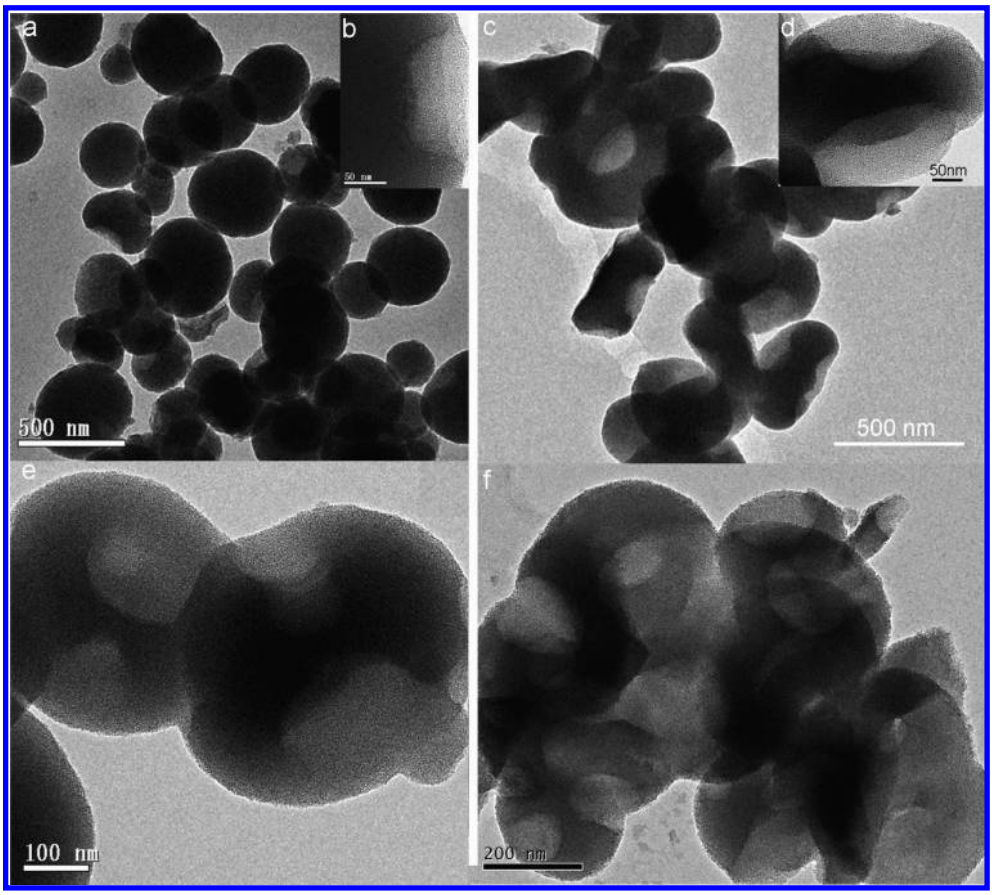

Figure 2. TEM images of four different mesoporous silica particles formed in the presence of R variation and calcinations at 550 °C for 5 h, (a,b) 2.40; (c,d) 1.20; (e) 0.60; (f) 0.3.

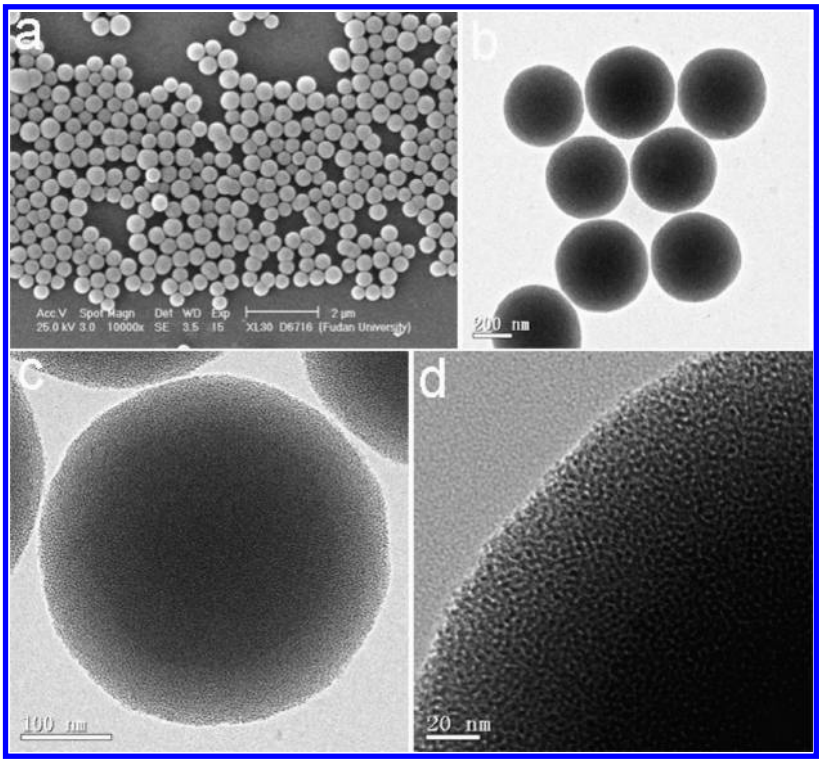

Figure 3. SEM images (a) and TEM images (b,c,d) of typically uniform mesoporous silica spheres formed after calcinations at 550 °C for 5 h; herein, $R = 0$.

mesoporous silica sphere with only one cavity in its surface can be obtained (Figure 2a,b). The sizes of the silica sample and its surface cavity are kept almost constant compared to the as-made samples (Figure 1a), respectively, indicating that the silica sphere undergoes little shrinkage during calcination. From Figure 2b, it can be clearly seen that the spherical silica sample exhibits well-defined porous features. At the same time, a novel monodisperse compressed bread-like mesoporous silica sample can also be observed in the case of R value of ~1.20 (Figure 2c,d). The calcined silica sample also exhibits obvious mesoporous features from Figure 2d; moreover, the size of opening of the cavity of the calcined silica sample is much larger than that of the as-made silica sample (Figure 2c). In addition, the maximum size of the cavity of the calcined sample was about 445 nm. However, novel mesoporous silica particles with multiple cavities can be observed in the case of $R \sim 0.6$ after calcination at 550 °C (Figure 2e). Additionally, the opening sizes of the cavities were almost constant compared to that of the as-made silica sample. The shape of cavities of the samples was well retained, indicating rigid framework of the silica sample. When the R value decreased to 0.3, multiple uniform cavities on mesoporous silica particles can be formed, as shown in Figure 2f, and it was found that the silica particles possess an obvious mesopore channel feature. It suggests that these unique silica particles indeed possess higher cavity volume so as to carry many more guest molecules compared to the other silica samples mentioned above.

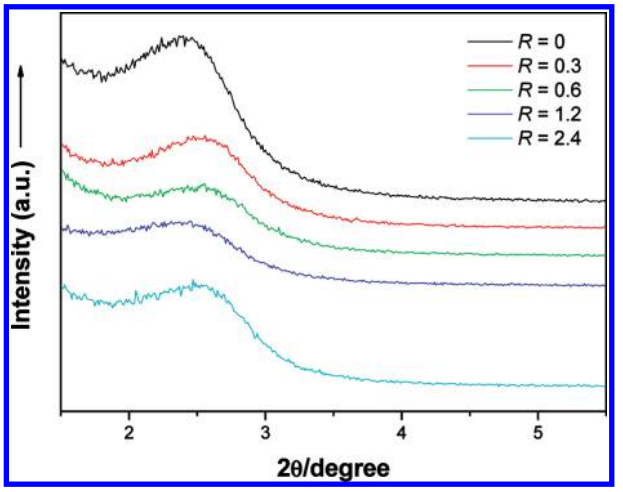

Figure 4. Small angle XRD patterns of the mesoporous silica particle samples formed in the presence of R value variation.

Table 2. Silica Samples Prepared from Different Mass Ratios of PAA to CATB (R)[a]

samples	R	D/ nm	S/ m^2/g	V/ cm^3/g
S0	0	2.08	736.1	0.2531
S1	0.3	2.15	891.3	0.2716
S2	0.6	2.14	850.6	0.2512
S3	1.2	2.08	780.4	0.2435
S4	2.4	2.25	740.6	0.2749

[a] D stands for the pore diameter calculated from the adsorption branch by BJH method, S is the BET surface area, and V represents pore volume.

At the same time, without PAA added, monodisperse mesoporous silica spheres can be obtained by calcination at 550 °C for 5 h (Figure 3). It was found that the calcined sample with R value of ~0 exhibits well-defined worm-like mesochannel features (Figure 3c,d). Notably, compared to the silica samples obtained in the presence of PAA template, no cavity is found on the surface of the mesoporous silica sphere synthesized without addition of PAA. It suggests that the PAA modifier can play a key role in mediating the formation of the cavity located on the silica particle surface.

Small-angle XRD patterns (Figure 4) of the calcined silica samples obtained at different R values show an obvious diffraction peak at ~2.5°. This could be indexed as a (100) plane of a mesostructure of *p6mm*. The broad diffraction peak suggests low ordering of the mesopores in the silica particles. The mean pore size calculated from the nitrogen adsorption branch by the BJH method is about 2.10 nm for the above five samples; the BET surface area was calculated to be ~891 m^2/g. For comparison, the physicochemical parameters of S0−S4 are listed in Table 2.

The nitrogen adsorption/desorption isotherms at 77 K for the mesoporous silica samples with distinct morphologies all show typical type-IV isotherms with a sharp capillary condensation step in the relative pressure range 0.85−0.95 (Figure 5A). In addition, pore size distribution curves (Figure 5B) of the five silica sample nanostructures were determined from the adsorption branch of the isotherms. All the pore size distributions exhibit a sharp peak centered at the mean value of around 2.10 nm, implying a uniform mesopore size. In addition, according to the

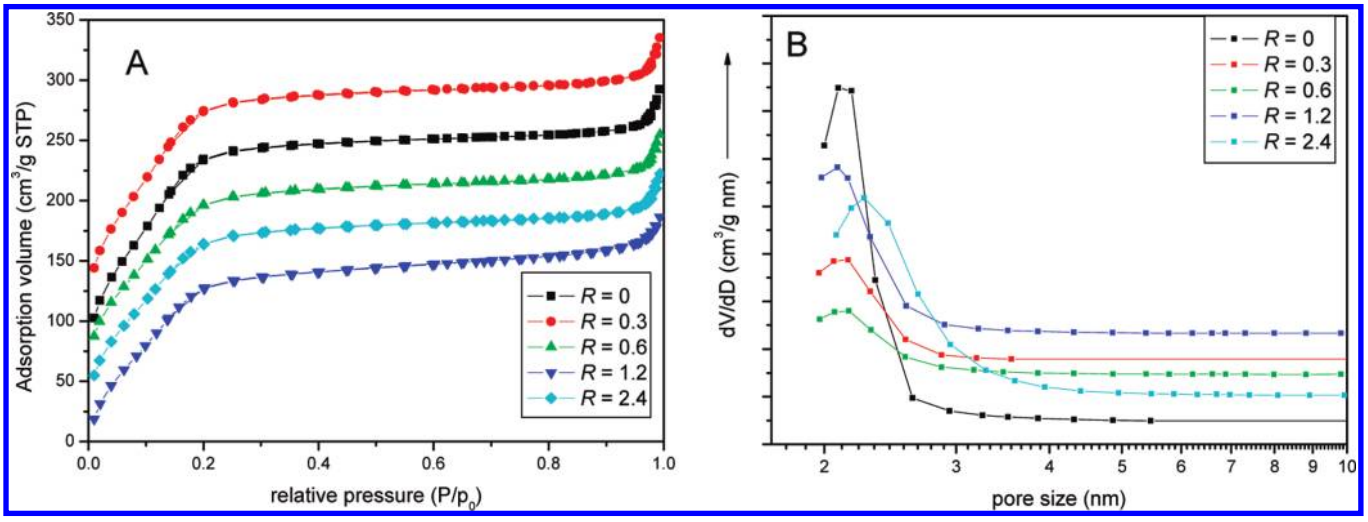

Figure 5. (A) N_2 adsorption−desorption isotherms and (B) pore size distribution curves of the calcined mesoporous silica particles formed in the presence of R value variation.

nitrogen adsorption−desorption results (Table 2), the addition of PAA has little effect on the mesoporosity of the obtained silica particles, including pore size, pore volume, and BET surface area of the silica sample. Their BET surface area and total pore volume are around 800 m^2/g and 0.25 cm^3/g, respectively.

Figure 6 shows the Fourier transform infrared (FT-IR) spectroscopy characterization results. For the as-made silica samples, the absorption bands observed in the region 2800−3000 cm^{-1} are attributed to the vibrations of $-CH_2$ of CTAB template, and the other two bands located in the regions 1725−1690 and 1440−1395 cm^{-1} are indexed as the vibration modes of C═O, O−H, and C−O of PAA modifier, respectively (Figure 6a). After calcination, no absorption peaks were observed in the ranges 2800−3000, 1725−1690, and 1440−1395 cm^{-1} for the mesoporous silica spheres (Figure 6b), suggesting that the CTAB and PAA templates can be almost completely removed through calcination treatment at 550 °C for 5 h.

Possible Formation Mechanism of the Hierarchical Silica Particles Proposed. On the basis of the above results, we speculate that the dramatic evolution of the morphology of the silica samples obtained with different amounts of PAA added should be closely related to the interactions among the PAA, CTAB, and silica oligomers during the aqueous sol−gel process. Due to the presence of PAA, the long PAA chain could couple the CTAB molecules via Coulomb force and electrostatic interaction to form spherical vesicles in solution. Moreover, the formed PAA/CTAB vesicle aggregates were stabilized by a specific oil/water interface that originated from the reduced solubility in isopropanol solvent system. Additionally, the majority of CTAB molecules are involved in the formation of the silica nanostructures. The self-assembly between silica oligomers and CTAB around the PAA/CTAB micellar aggregates took place very quickly to form various complex nanoarchitectures.

When a relatively larger amount of PAA is added, the larger PAA/CTAB spherical micellar aggregates undergo a volume swelling effect due to the electrostatic repulsion of the ionized PAA macromolecules. As the reaction proceeds, the isopropanol can gradually escape from the PAA/CTAB spherical micelle interface, which can destroy the stability of the interface layer of PAA/CTAB aggregates, and then, these hydrolyzed TEOS molecules can further cross-link around the destroyed surface of the large PAA/CTAB aggregates, which finally results in greater volume shrinkage for the whole sol−gel reaction system. Notably, the shrinkage effect will directly exclude the unstable PAA/CTAB micellar aggregate from the preformed silica framework that resulted from the reduction in surface area and surface free energy of the whole reaction system, as demonstrated in helical mesoporous silica structures that use PFOA and CTAB as co-surfactants,[23] which eventually resulted in the formation of silica particles with cavities on their surfaces. Particularly, the formation mechanism is completely consistent with the emulsion-mediated diffusion process for the preparation of the spherical silica particle with one hole on its surface.[21] However, when decreasing the amount of PAA added, the repulsion effect among these PAA molecules will decrease dramatically. Many more CTAB molecules can involve in the formation process of the PAA/CTAB micelle aggregates, where the CTAB can first form differently shaped micelles, and then the PAA can bind the CTAB micelle via electrostatic interaction to generate several PAA/CTAB aggregates. At the same time, the cross-linking polymerization of TEOS around the CTAB template simultaneously occurs around several different PAA/CTAB aggregate interfaces. Then, the evaporation of isopropanol continues to proceed, and the PAA/CTAB aggregates become totally unstable. With the cross-linking condensation reaction proceeding further, these PAA/CTAB micelles will finally be excluded from the preformed silica cross-linking framework due to reduction in

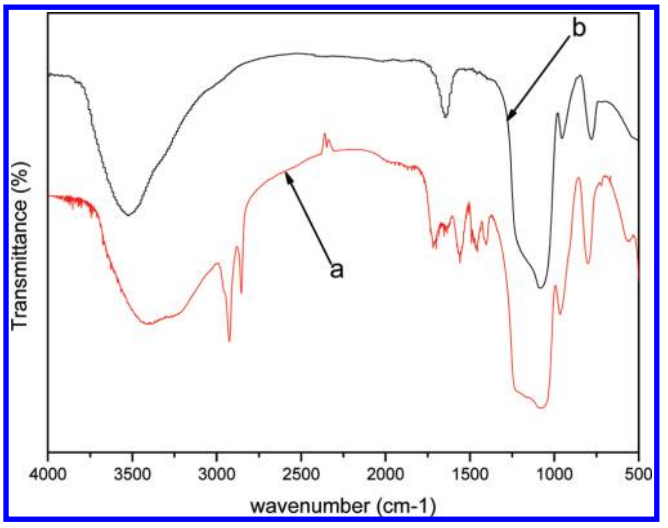

Figure 6. FT-IR spectrum of the silica samples obtained at different reaction conditions: (a) before calcination; (b) after calcination at 550 °C for 5 h.

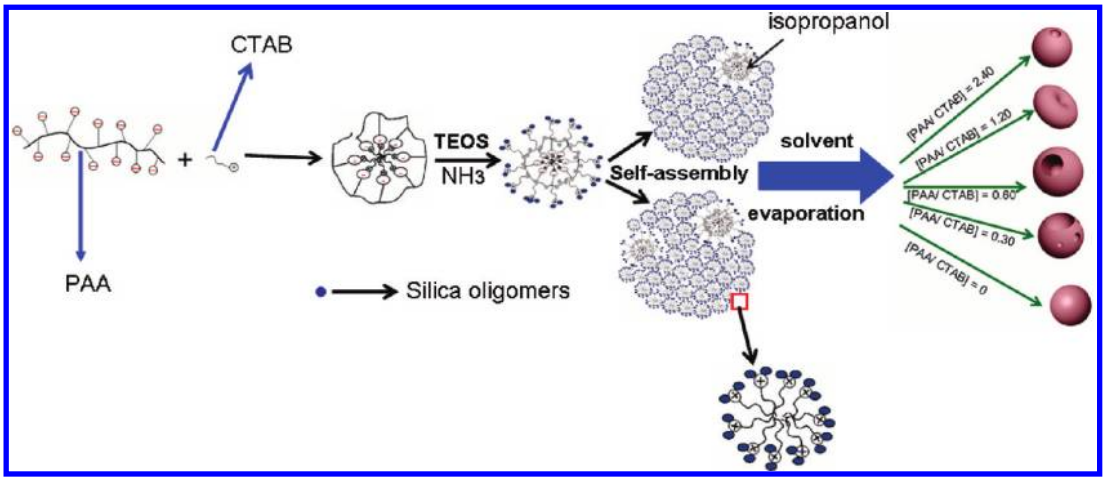

Figure 7. Schematic illustration of the hierarchically unique silica particles formed in the case of the mass ratios of PAA to CTAB variations.

the surface area and surface free energy of the whole system, which finally leads to the formation of silica particles with a different number of cavities in their surfaces. The whole formation process is shown in Figure 7. Therefore, the as-synthesized silica samples with tailored cavities may have resulted from the specific interface instability effect and the total reduction in the surface free energy. If no PAA was added, there is only the net electrostatic interaction between CTAB and silica oligomers, which can play a key role in forming the silica sphere. Clearly, the whole formation process of the as-synthesized silica particles with a cavity on the surface can also be further confirmed via investigating the early reaction process. Herein, we mainly explored the morphological evolution process of the sample of PAA/CTAB = 0.6 at the early reaction stage. When the reaction proceeds to 10 min, the as-obtained silica particles behave in almost monodisperse fashion and porous feature in its surface (Supporting Information Figure S4a), and the size of the cavity on its surface is about 10 nm. With the reaction prolonged, the as-synthesized silica particles partly aggregate with one another and distort the surface cavities; the size of the opening of these cavities can obviously be increased when reaction time reaches 45 min (Supporting Information Figure S4b). When the reaction time is increased to 2 h, the as-synthesized silica particles have formed a large amount of particle aggregates; even the smaller cavities from different particles can fuse to form larger cavities on their aggregate surfaces (Supporting Information Figure S4c). Results show that the Ostwald ripening process can be beneficial to formation of the varying cavity on the silica particle surface.

Conclusions

We have demonstrated that the anionic polymer PAA can be employed as a modifier for the formation of hierarchical silica nanostructures via a simple biosilification process in isopropanol and water solution, and various novel and unique mesoporous silica particles with adjustable cavities featured on their surfaces have been fabricated by changing the mass ratios of PAA to CTAB. Moreover, special mesoporous silica samples with specific cavities in their surfaces can be obtained through a facile sol−gel process using TEOS as the silica precursor, which makes it possible to further exploit their potential uses in catalysis, biological separation, and controlled drug delivery. In addition, the facile biomimetic synthesis strategy may promote the study of the biomineralization process and principle.

Acknowledgment. This work was supported by NSF of China (20421303, 20871030 and 20821140537), the State Key Basic Research Program of the PRC (2006CB0N0302). Shanghai Leading Academic Discipline Project (B108) and Shanghai Rising star program (08QA14010). XHG thanks China Postdoctoral Scientific Fund (20070420085) for financial support.

Supporting Information Available: Additional figures as described in the text. This material is available free of charge via the Internet at http://pubs.acs.org.